Glucagon Resistance and Decreased Susceptibility to Diabetes in a Model of Chronic Hyperglucagonemia

Nadejda Bozadjieva Kramer,[1,2,3] Camila Lubaczeuski,[4] Manuel Blandino-Rosano,[1,4] Grant Barker,[4] George K. Gittes,[5] Alejandro Caicedo,[4] and Ernesto Bernal-Mizrachi[4,6]

Diabetes 2021;70:477–491 | https://doi.org/10.2337/db20-0440

Elevation of glucagon levels and increase in α-cell mass are associated with states of hyperglycemia in diabetes. Our previous studies have highlighted the role of nutrient signaling via mTOR complex 1 (mTORC1) regulation that controls glucagon secretion and α-cell mass. In the current studies we investigated the effects of activation of nutrient signaling by conditional deletion of the mTORC1 inhibitor, TSC2, in α-cells (αTSC2^{KO}). We showed that activation of mTORC1 signaling is sufficient to induce chronic hyperglucagonemia as a result of α-cell proliferation, cell size, and mass expansion. Hyperglucagonemia in αTSC2^{KO} was associated with an increase in glucagon content and enhanced glucagon secretion. This model allowed us to identify the effects of chronic hyperglucagonemia on glucose homeostasis by inducing insulin secretion and resistance to glucagon in the liver. Liver glucagon resistance in αTSC2^{KO} mice was characterized by reduced expression of the glucagon receptor (GCGR), PEPCK, and genes involved in amino acid metabolism and urea production. Glucagon resistance in αTSC2^{KO} mice was associated with improved glucose levels in streptozotocin-induced β-cell destruction and high-fat diet–induced glucose intolerance. These studies demonstrate that chronic hyperglucagonemia can improve glucose homeostasis by inducing glucagon resistance in the liver.

Type 2 diabetes (T2D) and type 1 diabetes (T1D) are characterized by defective insulin action and insulin deficiency, respectively, both leading to hyperglycemia. However, another important component in regulation of glucose homeostasis is glucagon. In physiological states, glucagon plays a major role in maintaining glucose homeostasis by promoting glucose production via hepatic glycogenolysis and gluconeogenesis. Clinical data and animal experiments have shown that increased α-cell mass and glucagon secretion have a significant function in the pathogenesis of hyperglycemia in diabetes (1–6). In addition to the important role of glucagon in counterregulation of hypoglycemia, new evidence suggest that glucagon action could be used to lower glucose levels in diabetes by regulating insulin secretion and energy balance (7–10). Therefore, the current views on glucagon physiology are evolving and it is becoming clear that glucagon can be engaged in different physiological processes to regulate glucose homeostasis and energy balance (9).

Abnormal glucagon levels in individuals with T2D have been associated with the pathogenesis of hyperglycemia (11,12). The contribution of glucagon to hyperglycemia in diabetes was supported by lower glucose in mice with deletion of the glucagon receptor (GCGR) and in humans treated with GCGR antagonists (GRAs) (13–15). Increases in glucagon in T1D and T2D patients can also be explained in part by enhanced α-cell mass (3–5). Although the mechanisms leading to the rise in α-cell mass and glucagon levels in patients with diabetes are not fully understood, several hypotheses have been developed based on animal models. Mice fed with a high-protein diet or high-fat diet

[1]Department of Medicine, University of Michigan Medical Center, Ann Arbor, MI
[2]Division of Metabolism, Endocrinology and Diabetes, University of Michigan, Ann Arbor, MI
[3]Graduate Program in Cellular and Molecular Biology, University of Michigan, Ann Arbor, MI
[4]Division of Endocrinology, Metabolism and Diabetes, Department of Internal Medicine, Miller School of Medicine, University of Miami, Miami, FL
[5]UPMC Children's Hospital of Pittsburgh, University of Pittsburgh School of Medicine, Pittsburg, PA
[6]Veterans Affairs Medical Center, Miami, FL

Corresponding author: Ernesto Bernal-Mizrachi, ebernalm@med.miami.edu

Received 1 May 2020 and accepted 18 November 2020

This article contains supplementary material online at https://doi.org/10.2337/figshare.13256231.

N.B.K. and C.L. made equal contributions.

© 2020 by the American Diabetes Association. Readers may use this article as long as the work is properly cited, the use is educational and not for profit, and the work is not altered. More information is available at https://www.diabetesjournals.org/content/license.

(HFD) exhibit α-cell hyperplasia and hypertrophy, suggesting that nutrient environment and/or insulin resistance could regulate α-cell mass (16,17). In addition to the changes in α-cell mass, prolonged hyperinsulinemia in early stages of T2D could also induce α-cell insulin resistance with loss of suppression of glucagon release by insulin (18). Studies using liver-specific GCGR knockout mice highlighted the importance in the islet-liver axis and showed that circulating hepatic factors can increase α-cell proliferation independent of direct pancreatic input (19,20). The metabolomics profile in the GCGR knockout mice and experiments with GRA administration showed that increase in specific circulating amino acids is the major component driving the expansion in α-cell mass and glucagon levels (21–24). The rise in α-cell mass and proliferation in these models was sensitive to rapamycin, indicating that mTOR was implicated (22,25). Previous data from our laboratory demonstrated that mTOR complex 1 (mTORC1) signaling maintains postnatal α-cell mass and potentiates glucagon secretion during fasting in a K_{ATP} channel–dependent manner (26). These studies support the concept that changes in α-cell mass are regulated by extracellular signals including nutrients (amino acids, glucose) and growth factors (insulin). However, the molecular mechanisms driving α-cell mass expansion and hyperglucagonemia in conditions of T1D and T2D are not completely understood. Further, the physiological consequences of chronic and recurring hyperglucagonemia require further investigation for development of better novel interventions.

Lack of animal models of endogenous hyperglucagonemia has limited the physiological investigation of increased glucagon levels. In the present studies, we assessed the effects of hyperglucagonemia by intrinsic activation of mTORC1 in α-cells, without α-cell stimulatory signals such as GRAs or deletion of GCGR. We increased mTORC1 activity in α-cells by conditional deletion of TSC2, a negative mTORC1 regulator ($\alpha TSC2^{KO}$). Activation of mTORC1 signaling in α-cells provided a novel model for studying the consequences of chronic hyperglucagonemia in glucose homeostasis and liver metabolism.

RESEARCH DESIGN AND METHODS

Animals and Procedures

Mice were housed in a pathogen-free environment and maintained on a 12-h light/dark cycle in animal facilities at the University of Michigan and the University of Miami. The Glucagon-Cre mice (generous gift from Dr. G. Gittes at the University of Pittsburg) (27), expressing Cre recombinase driven by the glucagon promoter, were crossed with $TSC2^{flox/flox}$. These mice had mixed background between C57BL/6 and 129X1. A mix of both Glucagon-Cre and $TSC2^{flox/flox}$ or $TSC2^{flox/+}$ mice was used as controls. Littermate controls were used in all experiments to avoid potential effects from the genetic background. Reporter transgenic animals, CAG-tdTomato, were purchased from The Jackson Laboratory. In islet morphometric analysis, age-matched cohorts were used with male and female mice. Two-month-old male mice were fed with 60% HFD purchased from Research Diets (catalog no. D12492). Mice were treated with streptozotocin (STZ) (150 mg/kg; Sigma) by a single intraperitoneal (IP) injection at 2 months of age (28).

For the islet transplantation studies, 100 islets from $\alpha TSC2^{KO}$ and control mice were transplanted into the anterior chamber of one eye in nude mice (Envigo) as previously described (29,30). Overexpression of the mouse GCGR was achieved by adenoviral delivery in mice with intravenous injection in the tail vein of GCGR-expressing adenovirus (Ad-GCGR) (cat. no. AAV-259976) and Ad-CMV-Null (adenovirus containing control virus) (cat. no. 1300) (Vector Biolabs, Malvern, PA), dose of 1×10^9 pfu/10 g, as previously described (31,32). Fed insulin and glucagon levels were measured 4 days after adenovirus administration. Glucagon tolerance test (100 μg/kg) was performed 6 days after adenovirus administration. Liver and pancreata were collected 8 days after adenovirus administration. Daily administration of glucagon was performed by injection of exogenous glucagon (100 μg/kg) (Sigma-Aldrich) or saline (vehicle) in wild-type mice for 17 days. The blood samples for measurements of glucose and insulin levels were collected 30 min after daily glucagon injection.

Metabolic Studies

Body weight and random fed blood glucose were monitored monthly for a total of 3 months. Fed (9:00 A.M.) and fasting (12-h fast, 9:00 P.M.) glucose, insulin, and glucagon levels were evaluated in 2-month-old males. Blood was obtained from the tail vein, and blood glucose was measured with Accu-Chek blood glucose meter. IP glucose tolerance tests (2 g/kg) and insulin tolerance tests (ITT) (0.75 units/kg) were performed by IP injections of respective agents in male mice fasted for 6 h. Hepatic glucose production was measured by IP injection of pyruvate (2 g/kg) (Sigma-Aldrich) and glycerol (2 g/kg) (Amresco) in mice fasted for 16 h (for pyruvate) and male mice fasted for 4 h (for glycerol). Glucagon challenge was performed by IP injection of glucagon (100 μg/kg) (Sigma-Aldrich) in male mice fasted for 6 h. IP exendin 9-39 (Ex9) (50 μg/kg, cat. no. 4017799; Bachem) or vehicle (saline) was administered in fasted (4 h) control and $\alpha TSC2^{KO}$ mice 15 min prior to IP glucose challenge (2 g/kg). Food intake and activity levels were recorded for the duration of 3 days with use of Comprehensive Lab Animal Monitoring System metabolic chambers (Columbus Instruments). Lean body mass and fat mass were determined by DEXA (Lunar Pixi, Janesville, WI).

Hormone and Metabolite Measurements

Glucagon and insulin levels were measured with ELISAs (Mercodia and Alpco, respectively). The fed and fasted (12 h) plasma levels of active GLP-1 were measured with STELLUX Chemiluminescent Assay (cat. no. 80-GLP1A-CH01; Alpco). Prior to measuring of active GLP-1 levels,

DPP-IV Inhibitor (Millipore) was added to plasma before the samples were stored at −80°C. Total pancreatic glucagon was measured as previously described (26). Liver glycogen content was measured with glycogen assay (Sigma-Aldrich) with use of ~10 mg of liver samples according to the manufacturer's instructions. Plasma urea levels were measured with quantitative enzymatic Urea Assay Kit III (BioAssay Systems). Amino acids were measured with L-Amino Acid Quantitation Kit (Sigma-Aldrich).

Statistical Analysis

The statistical analysis for comparisons between two groups was performed by unpaired (two-tailed) Student *t* test. One-way ANOVA with post hoc Dunnett multiple comparisons test was used for comparisons of three or more groups with a common control. Two-way ANOVA with post hoc Tukey multiple comparisons test was used for comparisons of three or more groups without a common control. *P* values <0.05 were considered significant.

Study Approval

All protocols were approved by the University of Michigan and the University of Miami Animal Care and Use Committees and were in accordance with National Institutes of Health (NIH) guidelines.

Data and Resource Availability

Reagents and genetically modified mice developed in the context of this article will be shared with investigators from not-for-profit organizations who request them in accordance with institutional guidelines using a simple Material Transfer Agreement.

RESULTS

Mice With Gain of mTORC1 Signaling in α-Cells Exhibit Lower Fed Blood Glucose Levels Despite Hyperglucagonemia

α-Cell-specific deletion of TSC2 was achieved by crossing of Glucagon-Cre with $TSC2^{flox/flox}$ mice ($\alpha TSC2^{KO}$) (27,33). Phosphorylated S6 (serine 240) [pS6 (Ser^{240})] staining showed lack of mTORC1 activation in the majority of glucagon-positive cells after a 6-h fast in 2-month-old control mice (Fig. 1*A*). In contrast, pS6 (Ser^{240}) staining was preserved in glucagon-positive cells from $\alpha TSC2^{KO}$ mice, despite the same period of fasting (Fig. 1*A*). Assessment of pS6 (Ser^{240}) in glucagon-positive cells from dispersed islets using flow cytometry and quantitative mean fluorescence intensity (MFI) showed increased mTORC1 activity in α-cells from αTSC2KO mice (Fig. 1*B*). $\alpha TSC2^{KO}$ had lower body weight at 1 month of age, and the difference persisted until 3 months (Fig. 1*C*). The decrease in body weight in $\alpha TSC2^{KO}$ mice was attributed to enhanced locomotor activity and normal food intake (Supplementary Fig. 1*A–D*). In addition, recombination mediated by Glucagon-Cre was detected in the brainstem and hypothalamic regions (dorsomedial hypothalamic nucleus) and could have contributed to the changes in locomotor activity observed in $\alpha TSC2^{KO}$ mice (26) (Supplementary Fig. 1*E*). There were no significant differences in lean and fat mass between 2-month-old control and $\alpha TSC2^{KO}$ mice (Supplementary Fig. 1*F* and *G*). Random fed glucose levels were lower in $\alpha TSC2^{KO}$ compared with Glucagon-Cre; $TSC2^{flox/+}$ ($\alpha TSC2^{HET}$) and control mice (Fig. 1*D*). During fasting, glucose levels were comparable between the groups (Fig. 1*D*). Glucagon measurements in fed and 12-h-fasted mice were increased in $\alpha TSC2^{KO}$ mice (Fig. 1*E* and *F*). Fed insulin levels trended to be higher in $\alpha TSC2^{KO}$ mice compared with controls (Fig. 1*G*). No difference in insulin levels was observed after a 12-h fast (Fig. 1*H*).

$\alpha TSC2^{KO}$ Mice Exhibit α-Cell Hypertrophy and Hyperplasia and Increased Glucagon Content

$\alpha TSC2^{KO}$ mice were born with normal α-cell mass (Fig. 2*A*). Morphological evaluation in 2-month-old $\alpha TSC2^{KO}$ mice showed augmented α-cell size (Fig. 2*B* and *F*). The increase in cell size could also be observed by electron microscopy in 1-month-old $\alpha TSC2^{KO}$ mice (Fig. 2*C*). In addition, a higher number of glucagon granules was observed, and this was confirmed by elevation in total pancreatic glucagon content in 2-month-old $\alpha TSC2^{KO}$ mice (Fig. 2*D*). $\alpha TSC2^{KO}$ mice also showed expanded α-cell mass, α-cell size, α-cell number, and α-cell proliferation, with no changes in apoptosis at 2 months (Fig. 2*E–I*). $\alpha TSC2^{HET}$ mice showed no changes in α-cell mass compared with controls (data not shown). The pancreas weight normalized to body weight was reduced in $\alpha TSC2^{KO}$ mice compared with controls (Fig. 2*J*).

Glucagon, But Not GLP-1 Content, Is Increased in $\alpha TSC2^{KO}$ Mice

Since glucagon and glucagon-like peptide 1 (GLP-1) are generated from processing of proglucagon, we decided to assess GLP-1 levels in $\alpha TSC2^{KO}$ mice. No changes in fed and fasting active GLP-1 levels were observed in $\alpha TSC2^{KO}$ mice (Supplementary Fig. 2*A* and *B*). Assessment of glucagon content in sorted α-cells demonstrated increased content in $\alpha TSC2^{KO}$ islets (Supplementary Fig. 2*C*). Consistent with the normal levels in circulating GLP-1, active GLP-1 content in both isolated α-cells and small intestine was conserved in $\alpha TSC2^{KO}$ mice (Supplementary Fig. 2*D* and *E*). A nonsignificant trend toward higher glucagon content in the small intestine was observed in $\alpha TSC2^{KO}$ mice (Supplementary Fig. 2*F*). Examination of processing prohormone convertase 2 (PC2) revealed that PC2 appeared to be increased in $\alpha TSC2^{KO}$ mice compared with controls (Supplementary Fig. 2*G*). Staining for PC1/3 was low in both groups and difficult to quantify (data not shown). These findings show normal levels of active GLP-1 in plasma, α-cells, or small intestine and support the preference for glucagon processing in the α-cells of $\alpha TSC2^{KO}$ mice.

$\alpha TSC2^{KO}$ Mice Display Improved Glucose Tolerance and Increased Insulin Secretion

IP glucose tolerance testing revealed that $\alpha TSC2^{KO}$ mice displayed better glucose tolerance at 2 months compared with controls and $\alpha TSC2^{HET}$ mice (Fig. 3*A*). $\alpha TSC2^{KO}$ mice

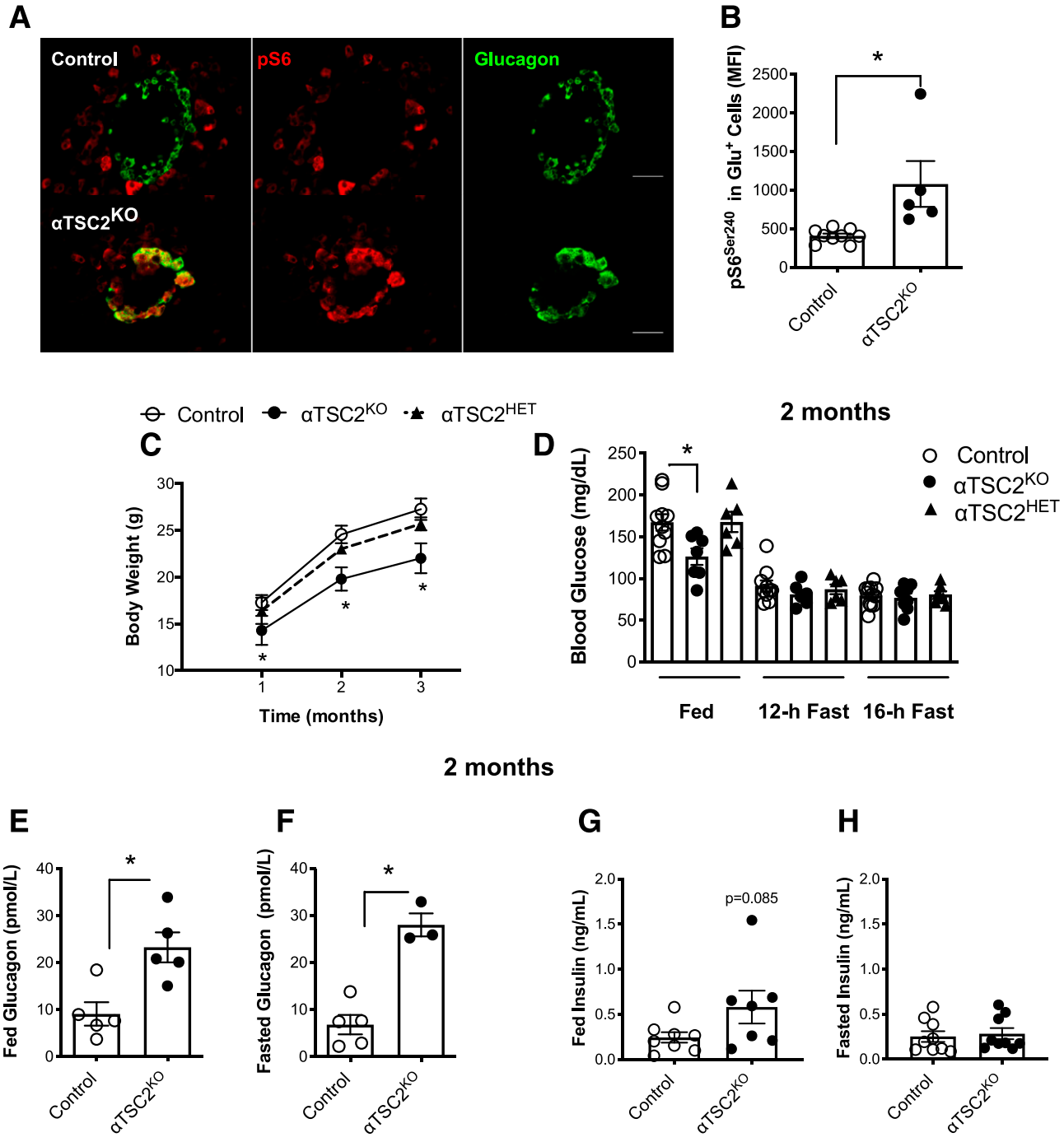

Figure 1—Mice with gain of mTORC1 signaling in α-cells exhibit lower fed blood glucose levels despite hyperglucagonemia. *A*: Immunofluorescent staining showing lack of positive mTORC1 activity [shown by pS6 (Ser^{240}) stain] in the control and the sustained mTORC1 activity in glucagon-positive cells of the $\alpha TSC2^{KO}$ mice in pancreas sections from control and $\alpha TSC2^{KO}$ mice after a 6-h fast ($n = 3$–4) (scale bar, 50 μm). *B*: Assessment of pS6 (Ser^{240}) staining by flow cytometry in glucagon-positive cells from control and $\alpha TSC2^{KO}$ islets ($n = 5$–9). *C*: Body weight of control, $\alpha TSC2^{KO}$, and $\alpha TSC2^{HET}$ mice ($n = 4$–8). *D*: Blood glucose in fed and fasting (12 h and 16 h) 2-month-old mice ($n = 6$–12). Fed ($n = 5$) (*E*) and fasted (12 h; $n = 3$–5) (*F*) glucagon levels. *G*: Fed insulin levels ($n = 7$–8). *H*: Fasted (12 h) insulin levels ($n = 9$). For *C* and *D*, data are shown as means ± SEM; $^*P < 0.05$ (one-way ANOVA with Dunnett posttest). For *B* and *E*–*H*, data are shown as means ± SEM; $^*P < 0.05$ (Student two-tailed *t* test). Glu, glucagon; hrs, hours; MFI, mean fluorescence intensity.

exhibited an increase in baseline insulin after a 6-h fast and enhanced insulin secretion after IP glucose challenge in $\alpha TSC2^{KO}$ mice (Fig. 3*B*). These data suggested that $\alpha TSC2^{KO}$ mice exhibit enhanced glucose tolerance due to increased insulin secretion (Fig. 3*A* and *B*). Next, we wanted to determine whether the improvement in glucose tolerance was due to increased glucagon-stimulated insulin secretion. Glucagon acts predominantly through β-cell

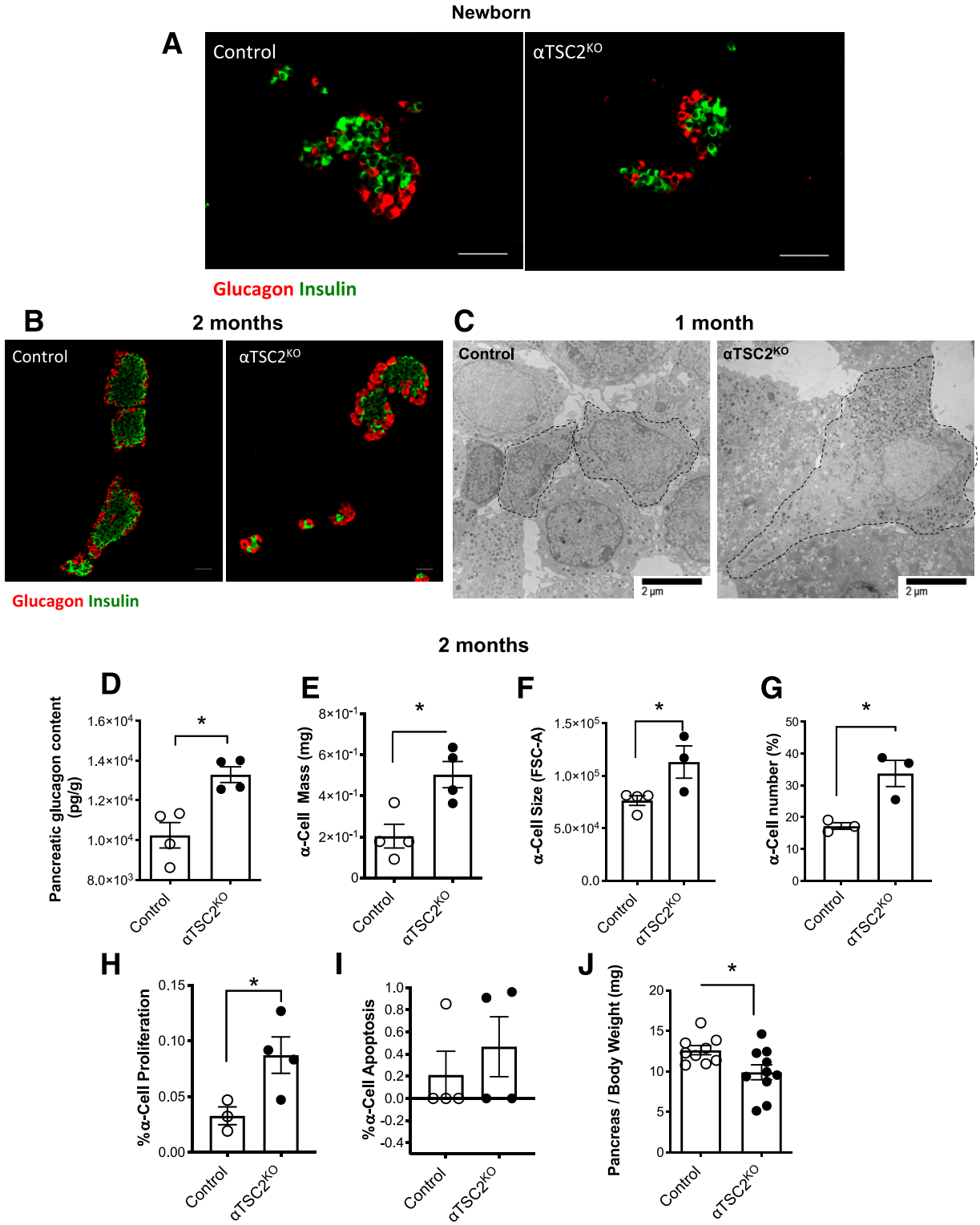

Figure 2—αTSC2^{KO} mice exhibit α-cell hypertrophy and hyperplasia and increased glucagon content. *A*: Immunofluorescent images of glucagon (red) and insulin (green) in pancreas at postnatal day 1 (scale bar, 50 μm). *B*: Immunofluorescent images of glucagon (red) and insulin (green) at 2 months (scale bar, 50 μm). *C*: Electron microscopy images from 1-month-old control and αTSC2^{KO} mice. *D*: Pancreatic glucagon content at 2 months ($n = 4$). *E*: Quantification of α-cell mass at 2 months ($n = 4$). Quantification of α-cell size ($n = 3$–4) (*F*) and quantification of α-cell number (*G*) by FACS (% of population from Glucagon-Cre; $^{CAG\text{-}tdTomato}$ (control) and αTSC2$^{KO;\ CAG\text{-}tdTomato}$ mouse islets; $n = 3$). The size of live glucagon (*F*) and insulin-positive cells (Fig. 3*E*) from dispersed islets was analyzed by flow cytometry and quantified by forward scatter area (FSC-A). Proliferation by positive ki67 and glucagon costain ($n = 3$–4) (*H*) and apoptosis by positive TUNEL and glucagon costain ($n = 4$) (*I*) in 2-month-old mice. *J*: Pancreas weight in 2-month-old mice ($n = 9$–10). Data for are shown as means ± SEM. *$P < 0.05$ (Student two-tailed *t* test).

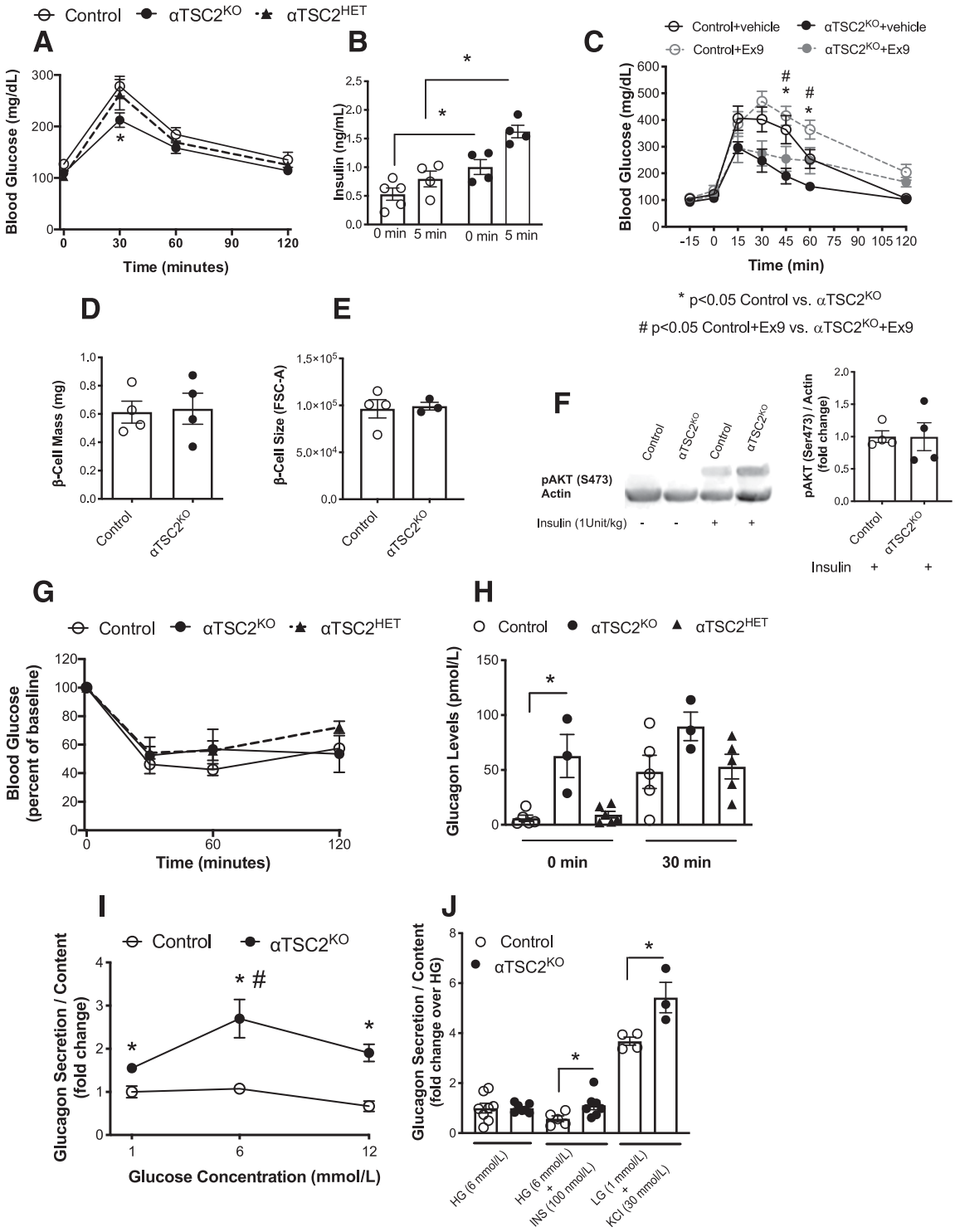

Figure 3—αTSC2^{KO} mice display improved glucose tolerance and increased insulin secretion. *A*: Glucose tolerance test (2 g/kg body wt) in 2-month-old mice ($n = 5$–8). *B*: Insulin levels at 0 and 5 min post–glucose administration (2 g/kg body wt) in 2-month-old mice ($n = 4$–5). *C*: Glucose tolerance test (2 g/kg body wt) in 2-month-old control ($n = 3$–4) and αTSC2^{KO} ($n = 6$) mice with preadministration of Ex9 (50 μg/kg, 15 min prior to glucose injection) or vehicle (saline). Quantification of β-cell mass (D) and β-cell size (*E*) in 2-month-old mice ($n = 3$–4). The size of live glucagon (Fig. 2*F*) and insulin-positive cells (*E*) from dispersed islets was analyzed by flow cytometry and quantified by forward scatter area (FSC-A). *F*: Western blot and quantification showing hepatic insulin sensitivity measured by phosphorylated AKT (pAkt) (Ser^{473}) after insulin administration in vivo (1 unit/kg) ($n = 4$ mice/group). Blood glucose response to ITT (0.75 units/kg body wt) (*G*) and glucagon response to ITT (0.75 units/kg body wt) (*H*) at 2 months ($n = 3$–6). Changes in blood glucose levels in response to insulin administration were reported as % change from 0 time point/baseline. *I*: Glucagon response from isolated islets to increasing glucose concentrations ($n = 5$–6 mice). *J*: Glucagon response from isolated islets to exogenous insulin (100 nmol/L) and KCl (30 mmol/L) (HG = 6 mmol/L glucose, LG = 1 mmol/L glucose; $n = 3$–8 mice). For *A*, *G*, and *H*, data are shown as means ± SEM; *$P < 0.05$ (one-way ANOVA with Dunnett posttest). For *C*, data are shown as means ± SEM; *$P < 0.05$ (two-way ANOVA with Tukey posttest). For *B*, *D*–*F*, *I*, and *J*, data are shown as means ± SEM; *$P < 0.05$ (Student two-tailed *t* test).

GLP1R to stimulate insulin secretion and exclusively on the GCGR in hepatocytes (7,8,34–36). Therefore, we blocked GLP1R by IP administration of Ex9 (50 μg/kg) in control and αTSC2^{KO} mice 15 min prior to IP glucose challenge. Glucose tolerance was improved in αTSC2^{KO} mice injected with vehicle control (Fig. 3*C*). Interestingly, differences in glucose excursions between control and αTSC2^{KO} mice persisted after administration of Ex9 (Fig. 3*C*). These data suggest that glucagon-induced insulin secretion was not the major mechanism for the differences in glycemia after a glucose challenge. The improved glucose tolerance and insulin secretion in αTSC2^{KO} mice were not associated with changes in β-cell mass or β-cell size (Fig. 3*D* and *E*). Assessment of liver insulin sensitivity by Akt phosphorylation after insulin administration in vivo showed similar levels of Akt phosphorylation (Ser^{473}) in αTSC2^{KO} mice, suggesting that hepatic insulin sensitivity was conserved (Fig. 3*F*). Assessment of insulin sensitivity and glucagon secretion by insulin-induced hypoglycemia showed that exogenous insulin administration caused a similar decrease in blood glucose levels in control αTSC2^{HET} and αTSC2^{KO} mice (Fig. 3*G*). Before insulin injection, glucagon levels were higher in αTSC2^{KO} mice compared with αTSC2^{HET} mice or control mice (Fig. 3*H*). A similar increase in glucagon secretion after insulin-induced hypoglycemia was observed in control and in αTSC2^{HET} mice (Fig. 3*H*). αTSC2^{KO} mice displayed a tendency to higher glucagon levels in response to insulin-induced hypoglycemia (Fig. 3*H*).

Assessment of Glucagon Secretion in Islets From αTSC2^{KO} and Control Mice

Exposure of islets to different glucose concentrations showed that control islets exhibited suppression of glucagon secretion as glucose levels in the media were changed from 1 to 12 mmol/L (Fig. 3*I*). In contrast, αTSC2^{KO} islets displayed higher glucagon levels at 1 mmol/L glucose, and glucagon secretion was induced after culture in 6 mmol/L and 12 mmol/L glucose, suggesting that inhibition of glucagon secretion by glucose was impaired in these mice (Fig. 3*I*). To uncover the mechanisms responsible for this response, we first assessed the effect of exogenous insulin in repressing glucagon secretion. Glucagon secretion remained higher in αTSC2^{KO} islets compared with control islets after insulin treatment (Fig. 3*J*). Examination of glucagon secretion in response to depolarization induced by potassium chloride (30 mmol/L KCl) showed that glucagon secretion was increased in αTSC2^{KO} islets (Fig. 3*J*). These data demonstrate that α-cells from αTSC2^{KO} mice are resistant to the inhibition of insulin in glucagon secretion, exhibit paradoxical increase in glucagon secretion in response to glucose, and secrete more glucagon after cell depolarization.

αTSC2^{KO} Mice Have Decreased Hepatic Glucagon-Induced GCGR Signaling

The experiments with Ex9 studies and the lack of hyperglycemia in mice with chronic hyperglucagonemia suggested the possibility of a defect in glucagon signaling in the liver of αTSC2^{KO} mice. To explore this further, we designed several experiments for examination of the effects of glucagon action in the liver of αTSC2^{KO} mice. Assessment of gluconeogenesis by pyruvate and glycerol tolerance tests revealed that hepatic glucose production was blunted in αTSC2^{KO} mice, indicating abnormal gluconeogenesis (Fig. 4*A* and *B*). Examination of glucagon signaling activation by exogenous glucagon injection showed that glucose excursion after glucagon administration was decreased in αTSC2^{KO} mice (Fig. 4*C*). Assessment of genes involved in glucagon signaling and gluconeogenesis showed that hepatic mRNA expression of GCGR, PEPCK, and glucokinase (Gck) were decreased in fed and fasted αTSC2^{KO} mice (Fig. 4*D* and *F*). No changes were observed in the hepatic mRNA levels of glucose 6-phosphatase (G6Pase) and fatty acid synthase (FAS) in fed and fasted states (Fig. 4*D* and *F*). Fed and fasted liver glycogen content in αTSC2^{KO} and control mice was also similar (Fig. 4*E* and *G*). To validate whether the reduction in GCGR expression was associated with decrease canonical GCGR signaling pathways, we examined hepatic CREB phosphorylation (pCREB) at Ser^{133} in response to exogenous glucagon injection (100 μg/kg) directly into the portal vein of fasted anesthetized mice. pCREB (S133) in liver lysates collected at baseline (fasted, 0 min) and post–glucagon treatment showed that control mice exhibited increased pCREB (S133) after 5 and 10 min of glucagon injection (Fig. 4*H*). In contrast, glucagon failed to increase pCREB in liver lysates from αTSC2^{KO} mice (Fig. 4*H*). These data are consistent with decreased hepatic glucagon-induced GCGR signaling in αTSC2^{KO} mice. Another important function of glucagon action in the liver is the increase in amino acid uptake, metabolism, and urea production (35). Assessment of genes involved in the amino acid metabolism showed that hepatic RNA expression of CREB-regulated transcription coactivator 2 (Crtc2) and glutamate pyruvate transaminase (GPT) was decreased in fasted αTSC2^{KO} mice (Fig. 4*I*). In addition, assessment of urea production in αTSC2^{KO} mice and control mice demonstrated that urea levels in circulation were decreased in αTSC2^{KO} mice (Fig. 4*J*). Finally, circulating L-amino acid levels were comparable in αTSC2^{KO} mice after fasting and in the fed state, indicating that this is not the cause of a decrease in ureagenesis (Fig. 4*K*).

Transient and Repetitive Hyperglucagonemia Induces Glucagon Resistance in Wild-Type Mice

To assess whether hyperglucagonemia is sufficient to downregulate GCGR signaling in the liver, we used two different approaches. First, transient and repetitive daily hyperglucagonemia by daily IP injections of glucagon or saline control showed that during the first 7 days, glucose levels (measured 30 min post–glucagon injection) were higher in glucagon-treated mice, consistent with the expected hyperglycemic responses to glucagon (Fig. 5*A*). However, after 9 days of glucagon treatment, glucose levels were similar to those of mice that received saline (Fig. 5*A*).

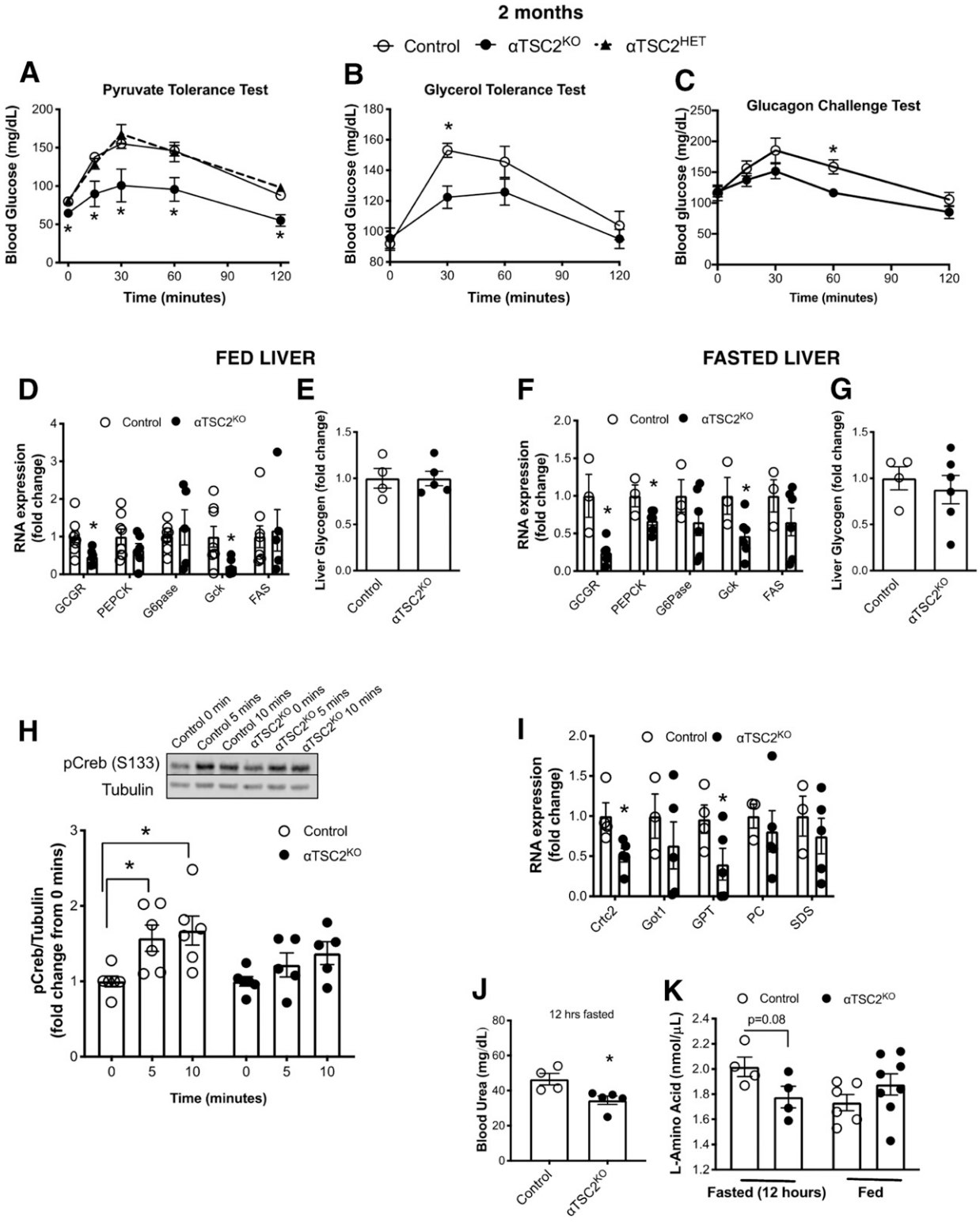

Figure 4—αTSC2^{KO} mice have decreased hepatic glucagon-induced GCGR signaling. *A*: Pyruvate tolerance test (2 g/kg) in 2-month-old mice after 16-h fast (n = 3–6). *B*: Glycerol tolerance test (2 g/kg) in 2-month-old mice after 6-h fast (n = 6–10). *C*: Glucagon challenge test (100 μg/kg) in 2-month-old mice after 6-h fast (n = 4–6). Fed liver mRNA levels of GCGR, PEPCK, G6Pase, Gck, and FAS (n = 5–8) (*D*) and liver glycogen content (n = 4–5) (*E*). Fasted liver mRNA levels of GCGR PEPCK, G6Pase, Gck, and FAS (n = 3–6) (*F*) and liver glycogen content (n = 4–6) (*G*). *H*: Exogenous glucagon (100 μg/kg) was directly injected into the portal vein of fasted control and αTSC2^{KO} anesthetized mice. pCREB (Ser^{133}) in liver lysates collected at baseline (fasted, 0 min) and 5 and 10 min post–glucagon injection. *I*: Fasted liver mRNA levels of Crtc2, glutamate oxaloacetate transaminase (Got1), GPT, pyruvate carboxylase (PC), and serine dehydratase (SDS) (n = 4–5). *J*: Fasted blood urea levels in 2-month-old mice (n = 4–5). *K*: Circulating L-amino acid levels in fasted (12 h) and fed mice (n = 4–8). Data for *A* are shown as means ± SEM; *$P < 0.05$ (one-way ANOVA with Dunnett posttest). Data for *B–K* are shown as means ± SEM; *$P < 0.05$ (Student two-tailed t test). hrs, hours.

Fed insulin levels were higher in glucagon-injected mice on day 17 of injections (Fig. 5*B*). More importantly, daily glucagon injection for 17 days was sufficient to downregulate hepatic GCGR expression (Fig. 5*C*). In the second model, we assessed hepatic GCGR expression by inducing chronic hyperglucagonemia in mice using a model of transplantation of islets from αTSC2^{KO} or control mice into the anterior chamber of the eye of nude mice (Fig. 5*D*). The mice that received transplantation islets from αTSC2^{KO} mice had increased glucose levels for the first 15 days posttransplantation (Fig. 5*D*). After 15 days, glucose in mice transplanted with αTSC2^{KO} islets returned to the levels observed in mice transplanted with control islets (Fig. 5*D*). Fasting glucagon levels were increased at day 9 in mice transplanted with islets from αTSC2^{KO} mice, and hyperglucagonemia was maintained after 27 days posttransplantation (Fig. 5*E*). Fed insulin levels were not different between the groups on day 27 posttransplantation (Fig. 5*F*). Assessment of liver GCGR mRNA demonstrated that mice transplanted with αTSC2^{KO} islets had decreased hepatic mRNA expression of the GCGR compared with mice transplanted with control islets (Fig. 5*G*). Recapitulation of the glucose abnormalities, hyperglucagonemia, and downregulation of the hepatic GCGR in mice transplanted with islets from αTSC2^{KO} mice also indicated that mTORC1 signaling in α-cells plays a more important role than central mTORC1 signaling in this metabolic phenotype.

Overexpression of the Hepatic GCGR in αTSC2^{KO} Mice Normalizes Blood Glucose Levels and Glucagon Tolerance

To further support our observations that downregulation of GCGR expression induced by chronic hyperglucagonemia contributes to the phenotype observed in αTSC2^{KO} mice, we overexpressed hepatic GCGR expression in αTSC2^{KO} mice. We administered intravenously Ad-GCGR or Ad-CMV-Null in αTSC2^{KO} mice. Ad-GCGR injection in αTSC2^{KO} mice was sufficient to increase hepatic GCGR levels 8 days following adenovirus administration (Fig. 6*A*) and normalized blood glucose levels to those of control mice 4 days post–adenovirus administration (Fig. 6*B*). Surprisingly, glucagon levels decreased in αTSC2^{KO}+Ad-GCGR mice and were comparable with those of control mice 4 days post–adenovirus administration (Fig. 6*C*). Insulin levels at the same time point trended higher than those in controls and were not different between αTSC2^{KO}+Ad-GCGR and αTSC2^{KO}+Ad-CMV-Null mice (Fig. 6*D*). Finally, a glucagon challenge test performed 6 days after adenovirus administration showed that αTSC2^{KO}+Ad-GCGR mice were able to respond to exogenous glucagon administration, similarly to control mice (Fig. 6*E*). In contrast, αTSC2^{KO}+Ad-CMV-Null mice were still glucagon resistant and showed no response in blood glucose levels after exogenous glucagon administration (Fig. 6*E*). Examination of multiple islets among different sections showed that α-cell mass in αTSC2^{KO}+Ad-GCGR mice appeared conserved in comparison with those of αTSC2^{KO}+Ad-CMV-Null mice despite a normalization of glucagon levels (Fig. 6*F*).

Hyperglycemia After STZ and HFD-Induced Glucose Intolerance Is Reduced in αTSC2^{KO} Mice

To test the effects of hyperglucagonemia in a model of insulin-deficiency, we administered high-dose STZ (150 mg/kg) by single injection to αTSC2^{KO} and control mice. Baseline blood glucose levels before STZ administration (6-h fast) were comparable between the two groups (Fig. 7*A*). Both groups had a rapid increase in blood glucose levels for 7 days after STZ, but αTSC2^{KO} mice maintained lower blood glucose (Fig. 7*A*). Control mice showed a trend of increased glucagon levels 7 days after STZ, but αTSC2^{KO} mice remained hyperglucagonemic before and after STZ administration (Fig. 7*B*). Control and αTSC2^{KO} mice exhibited undetectable insulin levels 7 days after STZ treatment (Fig. 7*B*). Analysis of islet morphometry revealed that αTSC2^{KO} mice maintained their higher α-cell mass, while the decrease in β-cell mass after STZ treatment was similar to that of control mice (Fig. 7*C–E*). These changes were also accompanied by increased α-cell size and a tendency to increase in α-cell proliferation in αTSC2^{KO} mice (Fig. 7*F* and *G*). Next, we tested the responses of hyperglucagonemia in αTSC2^{KO} mice in a model of diet-induced glucose intolerance by HFD. αTSC2^{KO} and control mice fed with 60% HFD for 4 weeks showed that αTSC2^{KO} mice gained weight comparable with controls (1.2-fold increase for controls and 1.4-fold increase for αTSC2^{KO}) but had lower fed and fasting blood glucose levels compared with controls (Fig. 7*H* and *I*). Fasting insulin levels were comparable between control and αTSC2^{KO} mice (Fig. 7*J*). As expected, control mice showed impaired glucose tolerance after HFD (Fig. 7*J*). In contrast, αTSC2^{KO} mice displayed improved glucose tolerance on control chow and were resistant to impaired glucose tolerance induced by administration of HFD for 4 weeks (Fig. 7*K*).

DISCUSSION

The current studies show that mTORC1 activation in islet α-cells results in chronic hyperglucagonemia as a result of α-cell mass expansion, increased glucagon content, and enhanced glucagon secretion. Surprisingly, chronic hyperglucagonemia in αTSC2^{KO} results in improved glucose tolerance, lower glucose levels during fasting, and enhanced insulin secretion. Improvement in glucose tolerance and normoglycemia despite high glucagon levels in αTSC2^{KO} mice resulted at least in part from downregulation of the hepatic GCGR expression and glucagon signaling. We also demonstrated that chronic high glucagon levels induce downregulation of GCGR expression using two models of hyperglucagonemia. Finally, αTSC2^{KO} mice exhibited better glucose levels after STZ-induced β-cell destruction and were resistant to HFD-induced glucose intolerance. These studies uncovered novel aspects of glucagon biology in a unique model of chronic hyperglucagonemia.

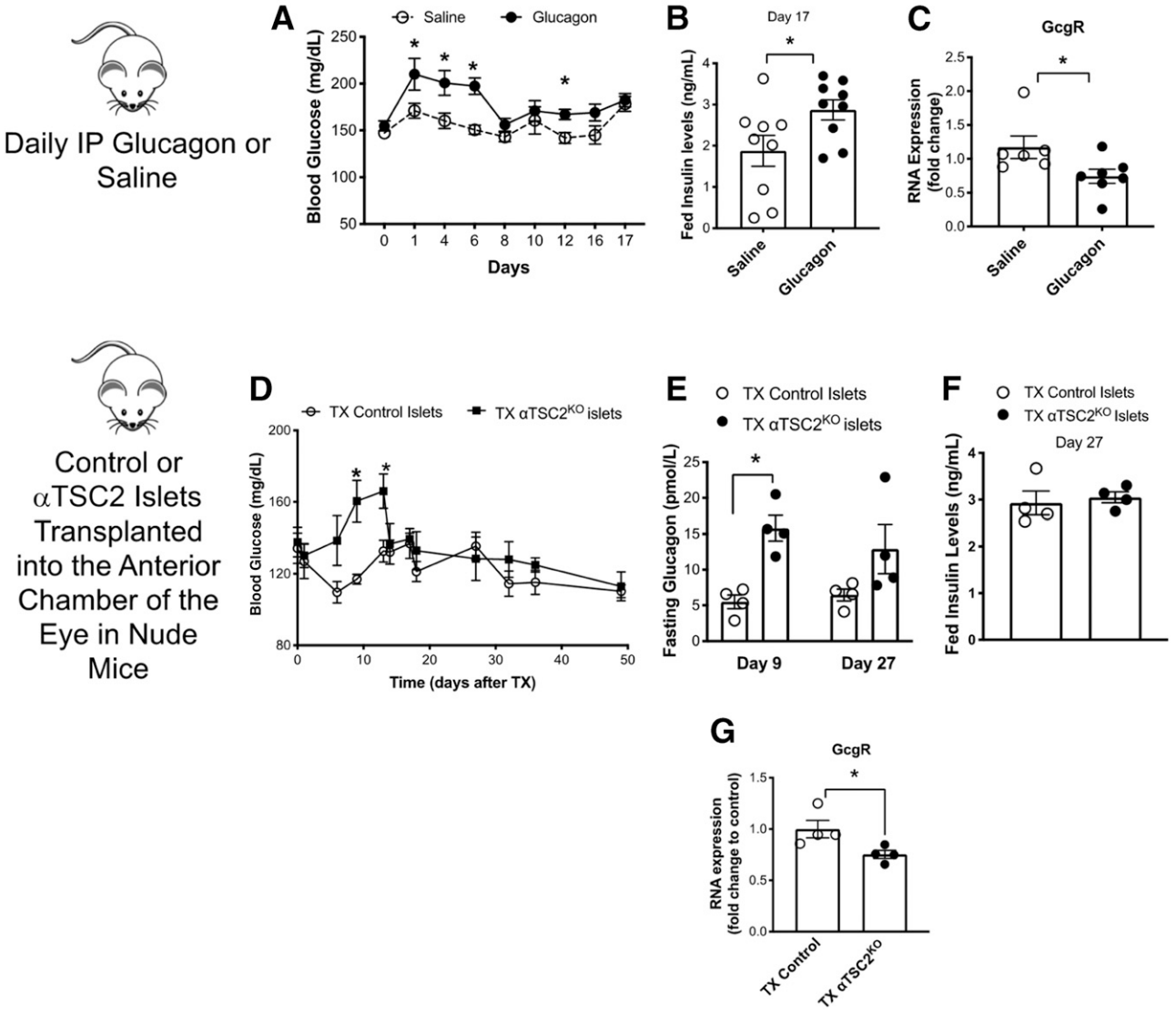

Figure 5—Transient and repetitive hyperglucagonemia induces glucagon resistance in wild-type mice. Fed glucose levels (*A*) and fed insulin levels (*B*) on day 17 after daily IP administration of glucagon (100 μg/kg) or saline ($n = 9$). *C*: Hepatic GCGR RNA expression levels in wild-type mice after daily IP administration of glucagon (100 μg/kg) or saline for 17 days ($n = 6$–7). Fed glucose levels ($n = 4$) (*D*), fasting glucagon levels (4 h) on day 9 and day 27 after transplantation ($n = 4$) (*E*), fed insulin levels on day 27 ($n = 4$) (*F*), and hepatic GCGR RNA expression levels (*G*) in nude mice transplanted with islets from $\alpha TSC2^{KO}$ or control mice into the anterior chamber of the eye ($n = 4$). Data are shown as means ± SEM. *$P < 0.05$ (Student two-tailed *t* test). TX, transplantation.

The current studies showed that increased mTORC1 activity in α-cells of $\alpha TSC2^{KO}$ mice was sufficient to induce postnatal α-cell mass expansion by increased proliferation and cell size. The changes in proliferation are consistent with the previous studies demonstrating reduction of α-cell proliferation by mTORC1 inhibition in α-cells (25,26). The increase in cell size in α-cells validates the increase in mTORC1 signaling. Interestingly, cell size and mass were conserved in β-cells, suggesting that potential Cre-mediated recombination in β-cells was minimal and not sufficient to induce changes in β-cell size and mass. In addition to the increase in mass, our studies support the concept that mTORC1 activation not only increases α-cell mass but also induces hyperglucagonemia by inducing constitutive glucagon secretion that was not suppressed by insulin and high glucose (Supplementary Fig. 3). In low glucose, $\alpha TSC2^{KO}$ islets exhibited higher glucagon secretion, and this was potentiated rather than inhibited by glucose (Supplementary Fig. 3). Interestingly, the increase in glucagon levels was not accompanied by changes in GLP-1 and preproglucagon processing in α-cells, as demonstrated by lack of changes in circulating active GLP-1 levels as well as conserved active GLP-1 content in isolated α-cells and small intestine between $\alpha TSC2^{KO}$ mice and controls (Supplementary Fig. 2). Future studies could be designed to further identify the stages in glucagon

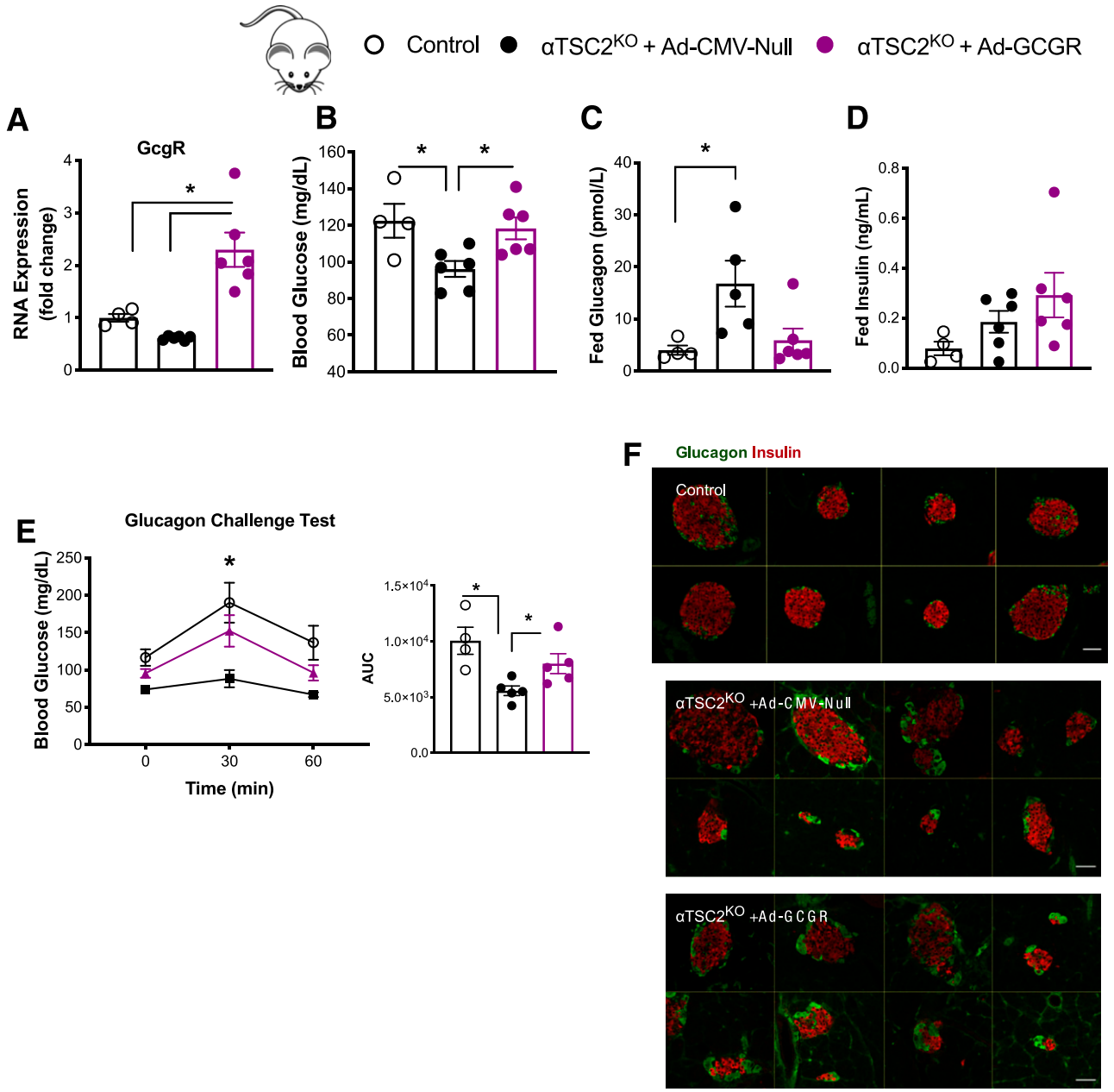

Figure 6—Overexpression of the hepatic GCGR in αTSC2^{KO} mice normalizes blood glucose levels and glucagon tolerance. Hepatic GCGR RNA expression levels 8 days after adenovirus administration (*A*) and fed glucose levels (*B*), fed glucagon levels (*C*), and fed insulin levels (*D*) in control, αTSC2^{KO}+Ad-GCGR, and αTSC2^{KO}+Ad-CMV-Null (control virus) mice 4 days after adenovirus administration (n = 4–6). *E*: Blood glucose response curve and area under the curve (AUC) after glucagon challenge test (100 μg/kg) in control, αTSC2^{KO}+Ad-GCGR, and αTSC2^{KO}+Ad-CMV-Null (control virus) mice (n = 4–5) 6 days after adenovirus administration. *F*: Glucagon and insulin staining in pancreas sections (scale bar, 50 μm). Data are shown as means ± SEM. *$P < 0.05$ (one-way ANOVA with Tukey posttest).

stimulus/secretion coupling regulated by mTORC1 signaling in α-cells.

Glucagon plays a major role in maintaining glucose homeostasis by promoting glucose production via hepatic glycogenolysis and gluconeogenesis. Clinical data have shown that α-cell mass and glucagon levels are elevated in patients who are insulin resistant or do not have diabetes and in T1D and T2D patients, leading to enhanced hepatic glucose output, and thereby exacerbate hyperglycemia (1–6). Contrary to this concept, hyperglucagonemia in αTSC2^{KO} mice was associated with reduced fed blood glucose levels and improved glucose homeostasis. Better glucose homeostasis in αTSC2^{KO} mice was in part explained by increased insulin secretion and conserved insulin sensitivity by liver AKT phosphorylation and glucose responses during ITT (Fig. 3). These results are in marked contrast to the improved insulin sensitivity observed after a single injection of glucagon agonists and suggest that acute effects

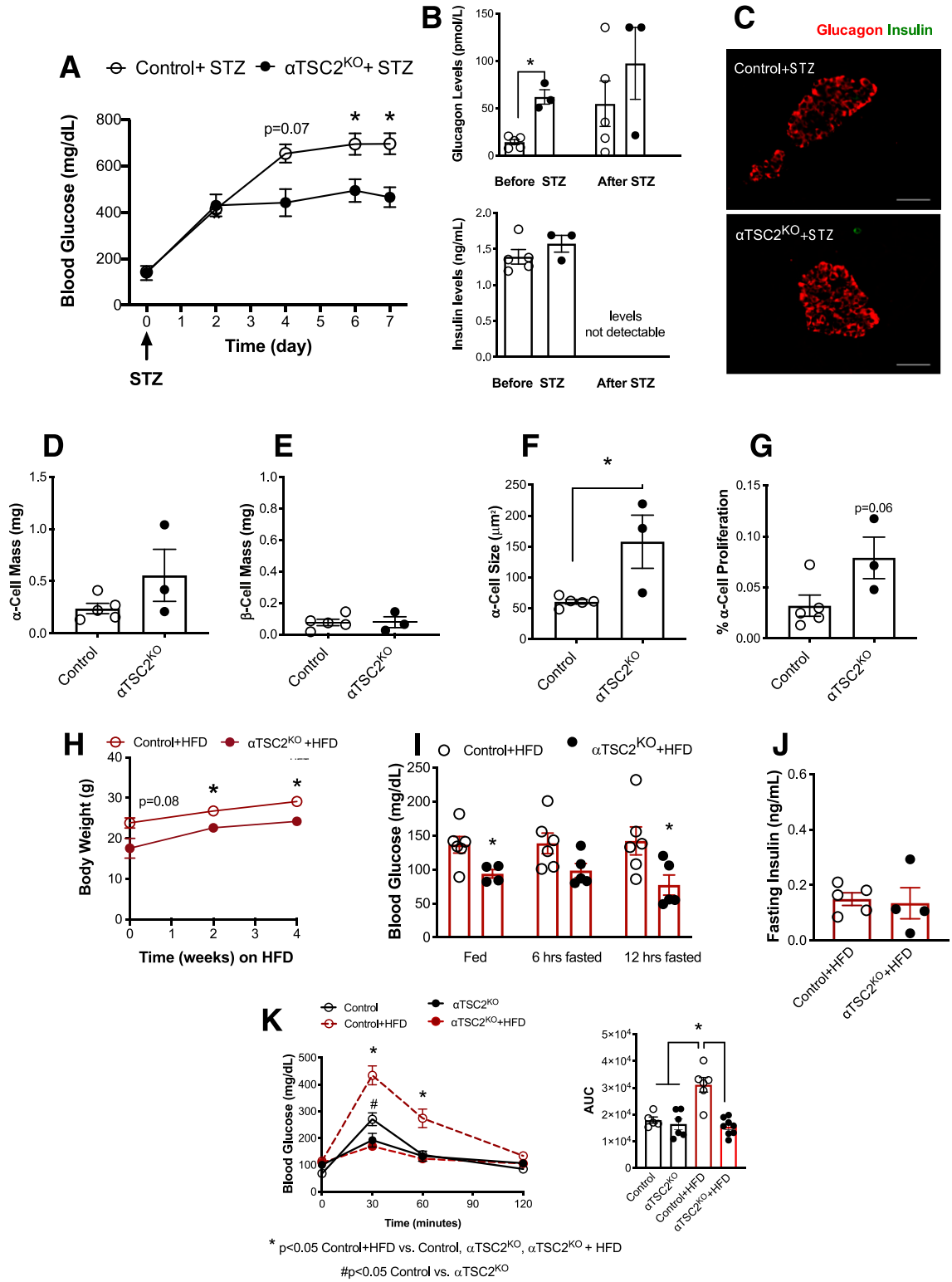

Figure 7—Hyperglycemia after STZ and HFD-induced glucose intolerance is reduced in αTSC2^{KO} mice. *A*: Fed blood glucose from day 0 to day 7 after single IP dose of 150 mg/kg STZ (n = 3–5). *B*: Circulating glucagon and insulin levels before (day 0) and 7 days after STZ (n = 3–5). *C*: Immunofluorescent images representing insulin (green) and glucagon (red) in pancreas sections from control and αTSC2^{KO} mice treated with STZ (scale bar, 50 μm). α-Cell (*D*) and β-cell (*E*) mass of mice after STZ (n = 3–5). α-Cell size (*F*) and α-cell proliferation (*G*) after STZ (n = 3–5). *H*: Body weight change after 4 weeks of HFD (n = 3–5). *I*: Blood glucose levels from fed and fasted (6 h and 12 h) 2-month-old mice after 4 weeks of HFD (n = 4–6). *J*: Fasted insulin levels after 4 weeks of HFD (n = 4–5). *K*: Glucose tolerance test (2 g/kg body wt) and area under the curve (AUC) in 2-month-old mice control and αTSC2^{KO} mice on chow diet or after 4 weeks of HFD (n = 5–8). For *A*–*J*, data are shown as means ± SEM; *$P < 0.05$ (Student two-tailed t test). For *K*, data are shown as means ± SEM; *$P < 0.05$ (two-way ANOVA with Tukey posttest). hrs, hours.

of glucagon on insulin sensitivity are lost after downregulation of GCGR expression during chronic hyperglucagonemia (37). Given that insulin sensitivity was conserved, we wanted to further evaluate the contribution of glucagon-stimulated insulin secretion and decreased hepatic glucose production as result of decreased hepatic GCGR. To assess this, we administered Ex9 to inhibit GLP1R and selectively reduce the effect of glucagon-mediated insulin secretion by acting on β-cell GLP1R. The results showed that the differences in glycemia between control and αTSC2^{KO} mice persisted after administration of Ex9 (Fig. 3*C*). These data suggested that the differences in glycemia are less likely the result of glucagon-induced insulin secretion.

Further validation that decreased gluconeogenesis and hepatic glucose production contribute to the improvement in glucose tolerance in αTSC2^{KO} mice was indicated by the response to pyruvate and glycerol challenge (Fig. 4). The lower hyperglycemic response to pyruvate, glycerol, and glucagon challenge was not explained by disturbances in liver glycogen content. These results suggested to us the possibility of abnormalities in glucagon action in the liver. Examination of GCGR expression in fed and fasted liver showed that GCGR expression was reduced in αTSC2^{KO} mice, implying that changes in gluconeogenesis and glucagon responses were caused by GCGR downregulation induced by chronic hyperglucagonemia. Decrease in GCGR expression was associated with reduction in glucagon-induced GCGR signaling as demonstrated by abnormal pCREB levels in liver lysates from αTSC2^{KO} mice injected with exogenous glucagon (Fig. 4*H*). Consistent with the decrease in glucagon action in the liver, we observed a reduction in the expression of gluconeogenic enzymes triggered by glucagon, such as *PEPCK*, and lower expression of *GPT* and *Crtc2* together with lower fasting plasma urea and a trend of lower plasma amino acid levels in circulation of αTSC2^{KO} mice. These data are consistent with decreased amino acid catabolism (Fig. 4).

The hypothesis that chronic hyperglucagonemia alone is sufficient to downregulate GCGR was further validated in in vivo studies in two models of chronic increase in glucagon by *1*) transient and repetitive daily hyperglucagonemia from IP injections of glucagon or saline in wild-type mice and *2*) constant hyperglucagonemia from transplanting of islets from αTSC2^{KO} or control mice into the anterior chamber of the eye in nude mice (Fig. 5). Exogenous daily glucagon injections or transplantation of αTSC2^{KO} islets resulted in early hyperglycemia. However, after 7 days of glucagon injection and 15 days after islet transplantation, fed blood glucose returned to the levels observed in controls. Interestingly, transient and repetitive hyperglucagonemia (glucagon injection) or constant hyperglucagonemia (islet transplantation) was sufficient to decrease hepatic RNA expression of the GCGR, suggesting that GCGR is downregulated relatively fast in states of hyperglucagonemia. Further evidence that GCGR downregulation plays a role in alteration of glucose homeostasis in αTSC2^{KO} mice comes from reconstitution studies by administration of Ad-GCGR or Ad-CMV-Null in αTSC2^{KO} mice. Intravenous Ad-GCGR in αTSC2^{KO} mice increased hepatic GCGR levels and normalized blood glucose to the levels of control mice and restored the response to exogenous glucagon. An interesting observation during these studies was a reduction in glucagon levels in αTSC2^{KO}+Ad-GCGR mice. α-Cell mass appeared to be conserved in αTSC2^{KO}+Ad-GCGR compared with that of αTSC2^{KO}+Ad-CMV-Null mice despite a normalization of glucagon levels (Fig. 6). This suggested that a more likely explanation is that increase in liver GCGR levels can increase plasma glucagon clearance as previously reported (38). Taken together, our studies support the concept that transient and repetitive hyperglucagonemia or chronic hyperglucagonemia from transplanted αTSC2^{KO} islets induces downregulation of the GCGR and a state of "glucagon resistance" in the liver. While some of the studies could be seen as underpowered, the use of different experimental approaches consistently supports our conclusion that chronic hyperglucagonemia downregulates liver GCGR signaling. Although these in vivo data are strongly suggestive of hepatic glucagon resistance in αTSC2^{KO} mice, additional studies are needed to fully elucidate the molecular mechanism.

Despite having high glucagon levels, αTSC2KO mice had better glycemic regulation in two mouse models of diabetes (Fig. 7). The improved hyperglycemia after STZ treatment in αTSC2^{KO} mice could be explained in part by reduction in liver GCGR expression and is reminiscent of observations in STZ-treated GCGR^{KO} mice (39–41). The lack of complete improvement in glucose after STZ treatment as described in GCGR^{KO} mice could be due to only partial reduction of GCGR expression (~50–70%) in the αTSC2^{KO} mice. We also tested the responses of hyperglucagonemia in αTSC2^{KO} in a model of diet-induced glucose intolerance by HFD. After 4 weeks of HFD, αTSC2^{KO} mice gained weight comparable with controls but had lower fed and fasting blood glucose levels compared with those of controls (Fig. 7). Most importantly, αTSC2^{KO} mice displayed improved glucose tolerance in control chow and were resistance to HFD-induced glucose intolerance. These data support the concept that partial downregulation of liver GCGR expression induced by hyperglucagonemia could play critical roles in controlling glucose homeostasis in models of type 1 and 2 diabetes.

Glucagon was viewed for centuries as insulin's counterregulatory hormone. Therefore, in the dogmatic view of glucagon it has been seen to raise blood glucose levels. It is accepted that hyperglycemic effects of glucagon are particularly important in acute states to defend the organism from the deleterious effects of hypoglycemia. At the same time, increased glucagon levels have also been linked to the pathogenesis of hyperglycemia in T2D. However, there is less understanding about the effects of chronic endogenous hyperglucagonemia on glucose homeostasis (9). Interestingly, pharmaceutical companies have developed GLP1R and CGCR coagonists as therapy for diabetes and obesity (9,42). These agents have been shown to

significantly improve glucose control and trigger weight loss in patients with T2D (43,44). These coagonists have favored GLP1R potency over GCGR potency and therefore are not a good model for understanding of the individual effect of chronic glucagon or chronic GCGR agonism in glycemia. Our studies are the first to show that chronic endogenous hyperglucagonemia in vivo controls glycemia by decreasing fed blood glucose levels, improves glucose tolerance, and downregulates hepatic GCGR expression. These studies shed light on our understanding of the effects of chronic hyperglucagonemia and offer a plausible explanation for the lack of hyperglycemic effects induced by GLP1R and CGCR coagonists. While chronic hyperglucagonemia is not observed in normal physiological states, these findings could provide some explanation of the changes in glucose homeostasis in pathological states of increased glucagon levels such as diabetes and glucagonomas. Further studies could assess the effects of these mechanisms after use of agents with dual GLP1R and GCGR activity.

Acknowledgments. The authors acknowledge Oliver Umland at the Flow Cytometry Core Facility (Diabetes Research Institute, University of Miami) and Alejandro Tamayo (University of Miami) for the tail vein injections for the adenovirus. The authors thank Drs. Mehboob Hussain, Charles Burant, Ken Inoki, John Williams, and Lei Yin (University of Michigan) for discussion of the data.

Funding. The authors acknowledge funding resources for this essential contribution to this work. E.B.-M. is mainly supported by a U.S. Department of Veterans Affairs Merit Review Award, no. IBX002728A . Additional funding includes NIH grants R01-DK073716 and DK084236. N.B.K. was supported by NIH grants T32GM007315, 5T32DK108740, and UL1TR002240. C.L. was supported by a Merit Review Award, no. IBX002728A, from the U.S. Department of Veterans Affairs and Diabetes Research Connection. The authors acknowledge support from the Morphology and Image Analysis Core, Metabolomics Core, and Phenotyping Core from the Michigan Diabetes Research Center (P30 DK020572).

Duality of Interest. No potential conflicts of interest relevant to this article were reported.

Author Contributions. E.B.-M. conceived, designed, and analyzed results and wrote the manuscript. N.B.K. and C.L. designed and performed the experiments, analyzed results, and wrote the manuscript. N.B.K., C.L., M.B.-R., and G.B. performed experiments and analyzed results. A.C. performed the islet transplantation into the anterior chamber of the eye. G.K.G. generated mice. All authors contributed to discussion and reviewed and edited the manuscript. E.B.-M. is the guarantor of this work and, as such, had full access to all the data in the study and takes responsibility for the integrity of the data and the accuracy of the data analysis.

Prior Presentation. Data from this study were presented in a plenary session at the 78th Scientific Sessions of the American Diabetes Association, Orlando, FL, 22–26 June 2018.

References

1. Dinneen S, Alzaid A, Turk D, Rizza R. Failure of glucagon suppression contributes to postprandial hyperglycaemia in IDDM. Diabetologia 1995;38:337–343

2. Sherwin RS, Fisher M, Hendler R, Felig P. Hyperglucagonemia and blood glucose regulation in normal, obese and diabetic subjects. N Engl J Med 1976;294:455–461

3. Orci L, Baetens D, Rufener C, et al. Hypertrophy and hyperplasia of somatostatin-containing D-cells in diabetes. Proc Natl Acad Sci U S A 1976;73:1338–1342

4. Rahier J, Goebbels RM, Henquin JC. Cellular composition of the human diabetic pancreas. Diabetologia 1983;24:366–371

5. Yoon KH, Ko SH, Cho JH, et al. Selective beta-cell loss and alpha-cell expansion in patients with type 2 diabetes mellitus in Korea. J Clin Endocrinol Metab 2003;88:2300–2308

6. Mezza T, Muscogiuri G, Sorice GP, et al. Insulin resistance alters islet morphology in nondiabetic humans. Diabetes 2014;63:994–1007

7. Zhu L, Dattaroy D, Pham J, et al. Intra-islet glucagon signaling is critical for maintaining glucose homeostasis. JCI Insight 2019;5:e127994

8. Capozzi ME, Svendsen B, Encisco SE, et al. β cell tone is defined by proglucagon peptides through cAMP signaling. JCI Insight 2019;4:126742

9. Finan B, Capozzi ME, Campbell JE. Repositioning glucagon action in the physiology and pharmacology of diabetes. Diabetes 2020;69:532–541

10. Svendsen B, Larsen O, Gabe MBN, et al. Insulin secretion depends on intra-islet glucagon signaling. Cell Rep 2018;25:1127–1134.e2

11. Wewer Albrechtsen NJ, Hartmann B, Veedfald S, et al. Hyperglucagonaemia analysed by glucagon sandwich ELISA: nonspecific interference or truly elevated levels? Diabetologia 2014;57:1919–1926

12. Müller WA, Faloona GR, Aguilar-Parada E, Unger RH. Abnormal alpha-cell function in diabetes. Response to carbohydrate and protein ingestion. N Engl J Med 1970;283:109–115

13. Johnson DG, Goebel CU, Hruby VJ, Bregman MD, Trivedi D. Hyperglycemia of diabetic rats decreased by a glucagon receptor antagonist. Science 1982;215:1115–1116

14. Kazda CM, Ding Y, Kelly RP, et al. Evaluation of efficacy and safety of the glucagon receptor antagonist LY2409021 in patients with type 2 diabetes: 12- and 24-week phase 2 studies. Diabetes Care 2016;39:1241–1249

15. Gelling RW, Du XQ, Dichmann DS, et al. Lower blood glucose, hyperglucagonemia, and pancreatic alpha cell hyperplasia in glucagon receptor knockout mice. Proc Natl Acad Sci U S A 2003;100:1438–1443

16. Morley MG, Leiter EH, Eisenstein AB, Strack I. Dietary modulation of alpha-cell volume and function in strain 129/J mice. Am J Physiol 1982;242:G354–G359

17. Ellingsgaard H, Ehses JA, Hammar EB, et al. Interleukin-6 regulates pancreatic alpha-cell mass expansion. Proc Natl Acad Sci U S A 2008;105:13163–13168

18. Liu Z, Kim W, Chen Z, et al. Insulin and glucagon regulate pancreatic α-cell proliferation. PLoS One 2011;6:e16096

19. Gromada J, Franklin I, Wollheim CB. Alpha-cells of the endocrine pancreas: 35 years of research but the enigma remains. Endocr Rev 2007;28:84–116

20. Longuet C, Robledo AM, Dean ED, et al. Liver-specific disruption of the murine glucagon receptor produces α-cell hyperplasia: evidence for a circulating α-cell growth factor. Diabetes 2013;62:1196–1205

21. Yang J, MacDougall ML, McDowell MT, et al. Polyomic profiling reveals significant hepatic metabolic alterations in glucagon-receptor (GCGR) knockout mice: implications on anti-glucagon therapies for diabetes. BMC Genomics 2011;12:281

22. Solloway MJ, Madjidi A, Gu C, et al. Glucagon couples hepatic amino acid catabolism to mTOR-dependent regulation of α-cell mass. Cell Rep 2015;12:495–510

23. Galsgaard KD, Winther-Sørensen M, Pedersen J, et al. Glucose and amino acid metabolism in mice depend mutually on glucagon and insulin receptor signaling. Am J Physiol Endocrinol Metab 2019;316:E660–E673

24. Kim J, Okamoto H, Huang Z, et al. Amino acid transporter Slc38a5 controls glucagon receptor inhibition-induced pancreatic α cell hyperplasia in mice. Cell Metab 2017;25:1348–1361.e8

25. Dean ED, Li M, Prasad N, et al. Interrupted glucagon signaling reveals hepatic α cell axis and role for L-glutamine in α cell proliferation. Cell Metab 2017;25:1362–1373.e5

26. Bozadjieva N, Blandino-Rosano M, Chase J, et al. Loss of mTORC1 signaling alters pancreatic α cell mass and impairs glucagon secretion. J Clin Invest 2017;127:4379–4393

27. Shiota C, Prasadan K, Guo P, et al. α-Cells are dispensable in postnatal morphogenesis and maturation of mouse pancreatic islets. Am J Physiol Endocrinol Metab 2013;305:E1030–E1040

28. Zhang Y, Zhang Y, Bone RN, et al. Regeneration of pancreatic non-β endocrine cells in adult mice following a single diabetes-inducing dose of streptozotocin. PLoS One 2012;7:e36675
29. Speier S, Nyqvist D, Köhler M, Caicedo A, Leibiger IB, Berggren PO. Noninvasive high-resolution in vivo imaging of cell biology in the anterior chamber of the mouse eye. Nat Protoc 2008;3:1278–1286
30. Speier S, Nyqvist D, Cabrera O, et al. Noninvasive in vivo imaging of pancreatic islet cell biology. Nat Med 2008;14:574–578
31. Lee Y, Berglund ED, Yu X, et al. Hyperglycemia in rodent models of type 2 diabetes requires insulin-resistant alpha cells. Proc Natl Acad Sci U S A 2014; 111:13217–13222
32. Asplin CM, Paquette TL, Palmer JP. In vivo inhibition of glucagon secretion by paracrine beta cell activity in man. J Clin Invest 1981;68:314–318
33. Hernandez O, Way S, McKenna J III, Gambello MJ. Generation of a conditional disruption of the Tsc2 gene. Genesis 2007;45:101–106
34. Chepurny OG, Matsoukas MT, Liapakis G, et al. Nonconventional glucagon and GLP-1 receptor agonist and antagonist interplay at the GLP-1 receptor revealed in high-throughput FRET assays for cAMP. J Biol Chem 2019;294:3514–3531
35. Wewer Albrechtsen NJ, Pedersen J, Galsgaard KD, et al. The liver-α-cell axis and type 2 diabetes. Endocr Rev 2019;40:1353–1366
36. Moens K, Flamez D, Van Schravendijk C, Ling Z, Pipeleers D, Schuit F. Dual glucagon recognition by pancreatic beta-cells via glucagon and glucagon-like peptide 1 receptors. Diabetes 1998;47:66–72
37. Kim T, Holleman CL, Nason S, et al. Hepatic glucagon receptor signaling enhances insulin-stimulated glucose disposal in rodents. Diabetes 2018;67: 2157–2166
38. Dobbins RL, Davis SN, Neal DW, Cobelli C, Jaspan J, Cherrington AD. Compartmental modeling of glucagon kinetics in the conscious dog. Metabolism 1995;44:452–459
39. Rivero-Gutierrez B, Haller A, Holland J, et al. Deletion of the glucagon receptor gene before and after experimental diabetes reveals differential protection from hyperglycemia. Mol Metab 2018;17:28–38
40. Lee Y, Wang MY, Du XQ, Charron MJ, Unger RH. Glucagon receptor knockout prevents insulin-deficient type 1 diabetes in mice. Diabetes 2011;60:391–397
41. Damond N, Thorel F, Moyers JS, et al. Blockade of glucagon signaling prevents or reverses diabetes onset only if residual β-cells persist. eLife 2016;5: e13828
42. Capozzi ME, DiMarchi RD, Tschöp MH, Finan B, Campbell JE. Targeting the incretin/glucagon system with triagonists to treat diabetes. Endocr Rev 2018;39: 719–738
43. Tillner J, Posch MG, Wagner F, et al. A novel dual glucagon-like peptide and glucagon receptor agonist SAR425899: results of randomized, placebo-controlled first-in-human and first-in-patient trials. Diabetes Obes Metab 2019;21:120–128
44. Ambery P, Parker VE, Stumvoll M, et al. MEDI0382, a GLP-1 and glucagon receptor dual agonist, in obese or overweight patients with type 2 diabetes: a randomised, controlled, double-blind, ascending dose and phase 2a study. Lancet 2018;391:2607–2618